Mechanisms of Photoresist Dissolution

Balazs Hunek and E. L. Cussler
Dept. of Chemical Engineering and Materials Science, University of Minnesota, Minneapolis, MN 55455

The comprehensive physical picture developed describes the dissolution of a broad range of materials, including novolak-based photoresists and can be applied to the dissolution in aqueous base of both small molecules and polymers that can ionize. The model was verified by measuring the dissolution of solute-coated spinning discs. Key experimental variables included the flow (as a Reynolds number) and the base concentration, which was in this case of sodium hydroxide. The physical and chemical characteristics of the dissolving species determine the rate-limiting steps, which cause different dissolution behavior. The dissolution of low molecular weight phenolic resin is controlled by a combination of solute release and solute mass transfer, without the formation of any significant intermediate gel phase. Several other dissolution mechanisms are rationalized based on a simple "strings of buoys" analogy, which can be extended to other cases as well.

Introduction

This article develops a comprehensive picture describing dissolution of a broad range of materials, including photoresists. The model applies to the dissolution in aqueous base of both small molecules and polymers that can ionize. Our experiments have included benzoic acid, novolak-based photoresists, and lithographic inks. Our model could be extended to other types of dissolving systems as well. Examples of such previously investigated systems include: (1) calcite dissolution in acetic acid (Fredd and Fogler, 1998); (2) asphaltene dissolution in amphiphile/alkane solutions (Permsukarome et al., 1997); and (3) the cleaning of calcium phosphate (Littlejohn et al., 2000), or behenic acid (Grant et al., 1996). In general, the physical and chemical characteristics of the dissolving species determine the rate limiting steps, which in turn cause different dissolution behavior.

What can happen during the dissolution is best seen from the phase diagram shown in Figure 1. Above the upper critical solution temperature (UCST) shown in Figure 1a, there can be two phases present: a pure solid solute phase R_s and a liquid solution. The solute concentration in solution varies from a high value $[R_i]$ (often near saturation), to a low concentration in the bulk liquid solution $[R]$. Below the UCST, an additional phase can appear between the liquid solution and the pure solid solute. This intermediate solute-rich phase, bounded by the concentrations $[R'_i]$ and $[R'_s]$, is sometimes called a "gel layer" or a "penetration zone" (Arcus, 1986; Peppas et al., 1994). Hence, critical solution behavior, which is closely related to molecular weight and solute-solvent interactions, plays a central role in determining the phases present during dissolution.

Dissolution in systems like these is described by a sequence of steps, depending on the characteristics of the system. For a low molecular weight simple solute like benzoic acid, there are two such steps. First, the solute dissolves. Second, it diffuses into the bulk solution. Such dissolution mechanisms have frequently been documented by experiments.

The aqueous dissolution of a high molecular weight water-soluble polymer such as xanthan and pectin is more complicated. It can be described by a three step sequence: (1) formation of a water swollen gel layer; (2) release of polymer from the gel layer; (3) transfer of the released polymer chains into the bulk solution (Parker et al., 2000). These dissolution steps correspond well with those of a heterogeneous reaction.

For insoluble solutes, the sequence of steps is still more complicated. One such example of interest here, is an insoluble solute, which reacts with an aqueous base to form a soluble species. Above the UCST, the dissolution of such a solute depends on a four-step mechanism. The steps are: (1) base transport to the solid; (2) acid-base reaction; (3) solute release from the solid phase; (4) solute transport into the solution. Above the UCST, these steps result in the concentration profile of Figure 1b.

Correspondence concerning this article should be addressed to E. L. Cussler. Current address of B. Hunek: Praxair Technology, Inc., Process & Systems R&D, CO_2 Technology, Tonawanda, NY 14150.

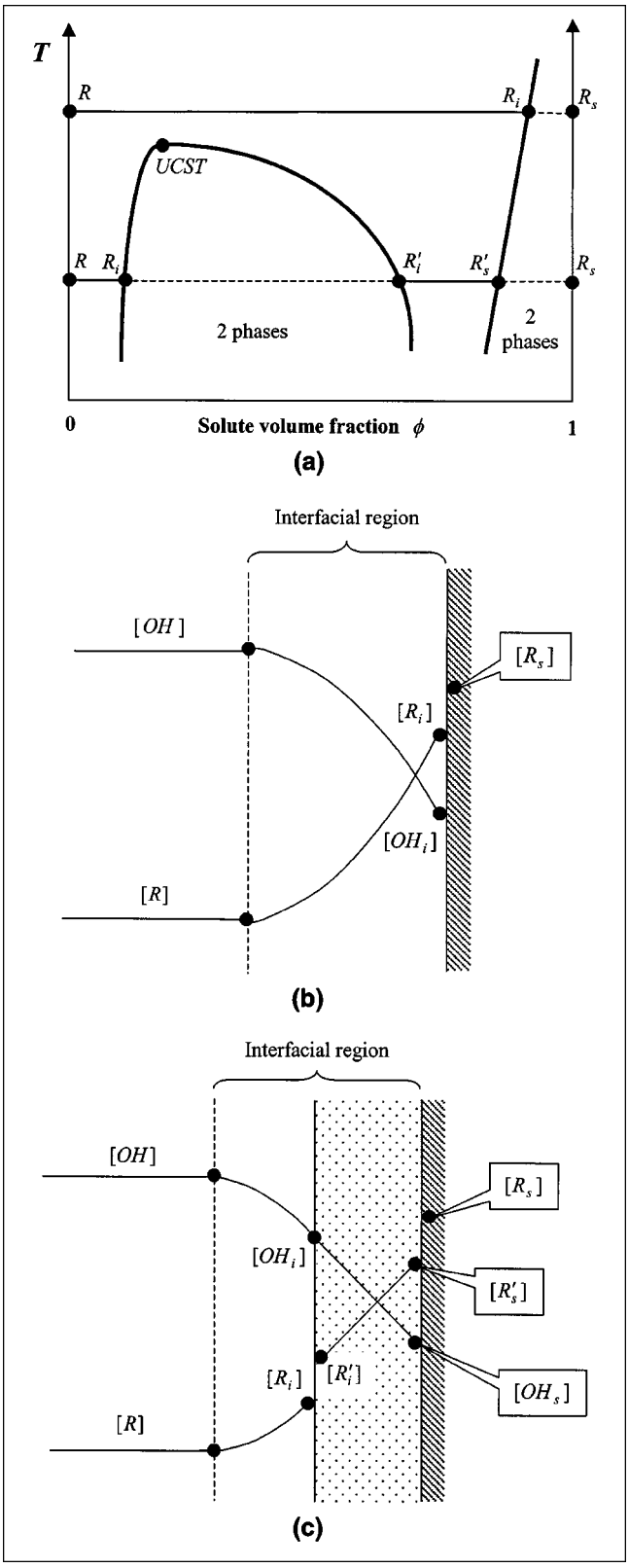

Figure 1. Possible phases during photoresist dissolution.

(a) Generalized solute-solvent phase diagram; (b) concentration profiles during dissolution above the upper critical solution temperature (UCST); (c) concentration profiles during dissolution below the UCST.

Dissolution in systems below the UCST involves a six-step mechanism, shown in Figure 1c. Base is transported first through the interfacial liquid (Step 1: $OH \rightleftharpoons OH_i$) and then across the intermediate solute-rich phase (Step 1′: $OH_i \rightleftharpoons OH_s$) to react with solid solute (Step 2). Step 3 includes the release of the conjugate base of the solute from the solid into the adjacent intermediate phase. This solute release is followed by transport to the bulk liquid in two sub-steps: through the intermediate phase (Step 4′: $R'_s \rightleftharpoons R'_i$) and finally from the surface of the intermediate phase into the bulk liquid (Step 4: $R_i \rightleftharpoons R$).

The overall dissolution rates depend on which steps of these sequences are slowest, and, hence, rate limiting. An extended discussion of these cases is given elsewhere (Hunek, 2000), so only a synopsis of experimentally relevant limits is given here. These include the case of benzoic acid, the case of water-soluble polymers, one case of a lithographic ink, and three cases for a resin like the novolak species. The benzoic acid case is the simplest: this forms no intermediate phase, and the dissolution is controlled by the diffusion of dissolved solute. When base is present, the total interfacial concentration of benzoic acid and benzoate is raised, but the rate-limiting step is unaltered.

Like some models for novolak resins, the case of water-soluble xanthan and pectin involves the formation of an intermediate gel phase, followed by the dissolution of single polymer chains. In the limit of high flow, the rate-controlling step is the release of polymer chains from the gel (Parker et al., 2000). In the case of the lithographic ink, an intermediate gel phase also forms (Bhaskarwar and Cussler, 1997). However, unlike the novolak and pectin cases, the ink gel layer is removed by shear as microscopic flakes, rather than the dissolution of large but single molecules. Thus, the control in this case is both physical and chemical. We will not discuss these cases further now, but will return to them in the discussion at the end of the article.

The more complex case of novolak resins is the subject of earlier theories. One earlier theory assumes that base diffusion can limit the dissolution rate when hydroxide ions slowly travel through an intermediate solute-rich phase (Arcus, 1986; Reiser et al., 1996). This intermediate phase is said not to form during the dissolution of low molecular weight novolaks that are important in photoresist formulation (Tsiartas et al., 1997). A second earlier theory can involve reaction control (Han and Reiser, 1998). A third theory assumes that dissolution can be limited by slow surface etching. The rate of etching is said to be proportional to the ratio of ionized to unionized phenolic sites of the solute (Tsiartas et al., 1997).

Our interpretation of low molecular weight novolak dissolution is different. We believe that the two slowest steps are solute release from the solid phase and diffusion of the dissolved species, without the formation of any significant intermediate gel phase. In other words, we believe that Steps 3 and 4 control dissolution. This proposal is one centerpiece of this article, and will be developed further below.

Theory

We believe that many dissolution processes, including that of novolak resins, are best explained by the sequence of dif-

fusion and reaction steps in Figure 1. In this section, we analyze in detail several limiting cases which turn out to be important experimentally. Before detailing these cases, we review the basis of our analysis.

First, we need a flexible nomenclature for our modeling. There are four important species participating in the dissolution: the hydroxide ion (OH); the counterion, such as sodium (Na); the acid function of a generic solute segment (RH), and the conjugate base of that segment (R). (We do not explicitly show the charges in order to simplify the notation.) Note that the last two chemical entities may represent either one molecule (as in the case of benzoic acid) or a repeat unit of a polymer chain (as in the case of phenolic resin).

We next consider equilibrium solubilities. Our solutes are subject to the dissociation equilibria of a weak acid and of water, and the overall electrical neutrality in the solution

$$[\mathrm{R}][\mathrm{H}] = K_a[\mathrm{RH}] \tag{1}$$

$$K_w = [\mathrm{OH}][\mathrm{H}] \tag{2}$$

$$[\mathrm{R}] + [\mathrm{OH}] = [\mathrm{H}] + [\mathrm{Na}] \tag{3}$$

Because the acid form of the solute is sparingly soluble, its concentration [RH] near equilibrium is essentially equal to its saturation value $[\mathrm{RH}]_{\mathrm{sat}}$. The concentration of the conjugate base of the solute [R] is found from the combination of these equations

$$[\mathrm{R}] = \frac{[\mathrm{Na}] + \sqrt{[\mathrm{Na}]^2 + 4(K_a[\mathrm{RH}]_{\mathrm{sat}} + K_w)}}{2\left(1 + \dfrac{K_w}{K_a[\mathrm{RH}]_{\mathrm{sat}}}\right)} \tag{4}$$

Since the sodium concentration is not altered by the acid-base reaction

$$[\mathrm{Na}] = [\mathrm{Na}]_o = [\mathrm{NaOH}]_o \tag{5}$$

Our experiments measure the total solute concentration in the solution $[\mathrm{R}]_T$, which is the sum of the acid and conjugate base forms

$$[\mathrm{R}]_T = [\mathrm{RH}] + [\mathrm{R}] = [\mathrm{RH}]_{\mathrm{sat}} + \frac{[\mathrm{NaOH}]_o + \sqrt{[\mathrm{NaOH}]_o^2 + 4(K_a[\mathrm{RH}]_{\mathrm{sat}} + K_w)}}{2\left(1 + \dfrac{K_w}{K_a[\mathrm{RH}]_{\mathrm{sat}}}\right)} \tag{6}$$

There are two important limits of this result. First, when sodium hydroxide is in excess, Eq. 6 simplifies to

$$[\mathrm{R}]_T = [\mathrm{RH}] + [\mathrm{R}] \cong [\mathrm{R}] = \frac{K_a[\mathrm{RH}]_{\mathrm{sat}}}{K_a[\mathrm{RH}]_{\mathrm{sat}} + K_w}[\mathrm{NaOH}]_o \tag{7}$$

Second, when little base is added, Eq. 6 becomes

$$[\mathrm{R}]_T = [\mathrm{RH}] + [\mathrm{R}] = [\mathrm{RH}]_{\mathrm{sat}}\left(1 + \frac{K_a}{\sqrt{K_a[\mathrm{RH}]_{\mathrm{sat}} + K_w}}\right) \tag{8}$$

These expressions are checked below for benzoic acid and novolak resins.

We now turn to the general dissolution sequence itself. In Step 1, hydroxide is transferred from the bulk liquid phase to the intermediate solute-rich phase

$$\mathrm{OH} \rightleftharpoons \mathrm{OH}_i \tag{9}$$

The rate is

$$r_1 = k_1 a([\mathrm{OH}] - [\mathrm{OH}_i]) \tag{10}$$

In Step 1′, hydroxide diffuses across the intermediate solute-rich phase to the reaction front

$$\mathrm{OH}_i \rightleftharpoons \mathrm{OH}_s \tag{11}$$

The rate is

$$r_{1'} = \frac{Da}{l}([\mathrm{OH}_i] - [\mathrm{OH}_s]) \tag{12}$$

Note that Step 1′ occurs only when an intermediate phase forms. Note also that Eq. 12 implies no partition coefficient (unity) between the intermediate phase and the bulk solution, a good approximation because the intermediate phase contains so much water (Cussler, 1997). In step 2, at the reaction surface, the acid and base react

$$\mathrm{OH}_s + \mathrm{RH}_s \rightleftharpoons \mathrm{R}_s + \mathrm{H_2O} \tag{13}$$

The rate is

$$r_2 = k_2[\mathrm{OH}_s][\mathrm{RH}_s] - k_{-2}[\mathrm{R}_s][\mathrm{H_2O}] \tag{14}$$

When this rate is fast, another step becomes rate-limiting; thus this step approaches equilibrium

$$[\mathrm{R}_s] = \frac{K_2}{[\mathrm{H_2O}]}[\mathrm{OH}_s][\mathrm{RH}_s] = K_2'[\mathrm{OH}_s][\mathrm{RH}_s] \tag{15}$$

In Step 3, the reacted solute dissolves: it gets released from the solid phase. At the same time, the dissolving solute uncovers another unreacted solute

$$\mathrm{R}_s \rightleftharpoons \mathrm{R}'_s + \mathrm{RH}_s \tag{16}$$

The rate is

$$r_3 = k_3[\mathrm{R}_s] - k_{-3}[\mathrm{R}'_s][\mathrm{RH}_s] \tag{17}$$

If this step is fast

$$[R'_s] = K_3 \frac{[R_s]}{[RH_s]} \tag{18}$$

The total number of lattice sites on a uniformly dissolving flat surface is fixed

$$[RH_s]_o = [RH_s] + [R_s] \tag{19}$$

so the surface contains both protonated and ionic groups.

Tangentially, this last equation makes us reconsider exactly what we mean by a release or a phase change of the reacted solute. This release may include the disentanglement or detachment of the ionized polymer chains (or its segments) from the unionized bulk polymer phase, the desorption of individual solute molecules, and the removal of solute by shear. The actual events depend on the dissolving species. However, in our experiments, we cannot tell exactly which species is involved. We can only measure the overall rate.

We now return to the overall mass-transfer mechanism, and, in particular, to the transport of the reacted and released species R'_s from the surface to the bulk solution. If no intermediate phase forms, $[R'_s]$ equals $[R_i]$, as shown in Figure 1a. If an intermediate phase does form, the next step (4′) is diffusion across this phase to an interfacial water-rich solution

$$R'_s \rightleftharpoons R'_i \tag{20}$$

The rate is

$$r_{4'} = \frac{D'a}{l}([R'_s] - [R'_i]) \tag{21}$$

Finally, in Step 4, solute is transferred from the interface with the bulk liquid into the bulk liquid itself

$$R_i \rightleftharpoons R \tag{22}$$

The rate is

$$r_4 = k_4 am\left([R_i] - \frac{[R]}{m}\right) \tag{23}$$

where m is the partition coefficient between the intermediate phase and the bulk solution.

We can use the equations above to predict how the dissolution rate varies with process conditions and stirring rate. Before doing so, we should reflect on two points about the intermediate phase which can be hard to appreciate. First, while we have assumed that solute diffuses across the intermediate phase in Step 4′, we could equally have assumed that water diffuses across this phase in the opposite direction. From that perspective, solute would be detaching from the solid interface in Step 3 at the same rate that solute is detached from the intermediate phase into the bulk solution in Step 4. Because the model is at steady state, the equations will still be the same.

The second point worthy of reflection is that no intermediate phase can form if Step 4 is fast. In the case we are discussing, the solute concentration in the bulk solution is always less than its solubility. If Step 4 is fast, then the interfacial concentration must equal the bulk, and so no intermediate phase can form (cf. Figures 1a and 1c). Conversely, if an intermediate phase does form, then mass transfer must be important, and Step 4 cannot be neglected. In this case, analyzing dissolution must include specifying the flow and other conditions in the bulk solution.

The mechanism above establishes a mathematical formalism for the dissolution. Based on this general mechanism, the dissolution rate will be derived next for two representative examples, benzoic acid and phenolic resin.

Example 1: benzoic acid

The case when solute mass transfer (Step 4) is the single rate-limiting step is common: many sparingly soluble solutes dissolve with this mechanism. No intermediate phases form. Benzoic acid is one example. In this case, the dissolution rate is just

$$\frac{d[R]}{dt} = k_4 a([RH_i] - [RH]) + k_4 a([R_i] - [R]) \tag{24}$$

The particular value of k_4 will depend on the physical situation involved, but will normally be almost equal for RH and for R.

When benzoic acid dissolves in aqueous base, the situation is more complicated because of the presence of benzoate. We are not sure where benzoate forms. For example, if benzoate forms only at the surface, the concentration profile of the dissolving system is as shown in Figure 1b. After considering fast base transport ($[OH] = [OH_i]$), we can combine Eqs. 15, 18, and 23 to find

$$\frac{d[R]}{dt} = k_4 a(K'_2 K_3 [OH] - [R]) \tag{25}$$

Alternatively, if the benzoate is formed in solution, then the dissolution rate will be proportional to the benzoic acid solubility, but the mass-transfer coefficient will be increased by the reaction in solution producing benzoate. This increase is proportional to the hydroxide concentration. Thus, the dissolution rate is (Cussler, 1997)

$$\frac{d[R]}{dt} = k_4 a([RH_i] + E[OH]_o - [R]) \tag{26}$$

where E is an enhancement factor due to chemical reaction. We will return to the meaning of the enhancement factor in the discussion section below.

Example 2: Novolak-based photoresist dissolution

The dissolution of phenolic resin will be shown to be a case of the combined control of solute release and solute mass transfer. This type of resin is the majority component of the

novolak-diazonaphthoquinone photoresist system (Reiser, 1989). Unlike benzoic acid, this resin is practically insoluble unless acid-base reaction ionizes the phenolic segments at the surface. The solubilization of fatty acids in aqueous detergent solutions is one close parallel (Chan et al., 1976; Kabin et al., 1996). The insoluble fatty acid dissolves in water as a mixed micelle formed by detergent surrounding the fatty acid. The dissolution includes micelle desorption and diffusion. These two processes are similar to the solute release (Step 3) and the mass transfer (Step 4) of resin dissolution. The key difference is the segmental ionization and release of the polymer chain, which occur repeat unit by repeat unit.

We can describe this dissolution using the equations given. For a low molecular weight resin, we assume no intermediate solute-rich phase formation (Tsiartas et al., 1997). Consequently, the ionized solute (the phenolate ion segment R_s) is released directly in the adjacent interfacial liquid R_i instead of an intermediate solute-rich phase R'_s (cf. Figure 1). The rate of dissolution under pseudo-steady-state conditions is found from Eq. 23

$$\frac{d[\mathrm{R}]}{dt} = r_4 = k_4 a([\mathrm{R}_i] - [\mathrm{R}]) \tag{27}$$

Because mass transfer of base from the bulk liquid to the liquid-solid interface is fast, [OH] equals $[\mathrm{OH}_i]$. Because the reaction between base and the phenolic acid groups of the resin is also fast (Atkins et al., 1995), the surface concentration $[\mathrm{R}_s]$ can be found by combining Eqs. 15 and 19

$$[\mathrm{R}_s] = \frac{K'_2[\mathrm{RH}_s]_o}{1 + K'_2[\mathrm{OH}]}[\mathrm{OH}] \tag{28}$$

If the rates of the slowest, thus rate-controlling, Steps 3 and 4 are assumed to be nearly equal, Eqs. 17 and 23 can be combined to give

$$k_3[\mathrm{R}_s] - k_{-3}[\mathrm{R}_i][\mathrm{RH}_s] = k_4 a([\mathrm{R}_i] - [\mathrm{R}]) \tag{29}$$

In this result, we have set $m = 1$ because there is no intermediate phase. Substitution of Eqs. 19 and 28 into 29 yields after rearrangement

$$[\mathrm{R}_i] = \frac{\dfrac{1}{k_4 a}[\mathrm{OH}] + \dfrac{1 + K'_2[\mathrm{OH}]}{k_3 K'_2[\mathrm{RH}_s]_o}[\mathrm{R}]}{\dfrac{1 + K'_2[\mathrm{OH}]}{k_3 K'_2[\mathrm{RH}_s]_o} + \dfrac{1}{k_4 a}\dfrac{1}{K'_2 K_3}} \tag{30}$$

This expression for the interfacial phenolate ion concentration $[\mathrm{R}_i]$ can be substituted back into Eq. 27

Table 1. Six Cases of Dissolution with Single Step Rate-Control*

Case No.	Rate-Controlling Step	Mass-Transfer Resistance $\frac{1}{Ka}$	Response to Flow (Spinning Disc Geometry)	Response to Hydroxide Conc.	Example Solute	Closest Parallel from Literature
1	S1—Reagent mass-transfer	$\frac{1}{k_1 a}$	$\frac{1}{Ka} \propto \frac{1}{\sqrt{Re}}$	None	Unlikely	
2	S1′—Reagent diff. in intermed. phase (IP)	$\frac{l}{Da}$	None	None	None known	Percolation model for novolak dissolution (Riser et al., 1996)
3	S2—Surface reaction	$\frac{1}{k_2[RH_s]_o}$	None	None	GaAs substrates	Semiconductor etching (Robertson and Fogler, 1996); Deprotonation reaction control of novolak dissolution (Han and Reiser, 1998)
4	S3—Solute release	$\frac{1 + K'_2[\mathrm{OH}]}{k_3 K'_2[RH_s]_o}$	None	$\frac{1}{Ka} \propto [\mathrm{OH}]$	Xanthan, Pectin	Dissolution of polymer powders (Parker et al., 2000); Surface etching model (Tsiartas et al., 1997)
5	S4′—Solute diff. in intermed. phase (IP)	$\frac{1}{D'a}\frac{1}{K'_2 K'_3}$	None	None	None known	
6	S4—Solute mass transfer	$\frac{1}{k_4 am}\frac{1}{K'_2 K_3}$	$\frac{1}{Ka} \propto \frac{1}{\sqrt{Re}}$	None	Benzoic acid	Heterogeneous reaction with mass transfer control (Levich, 1962)

*Case 6 is closest to our benzoic acid experiments.

$$\frac{d[\mathrm{R}]}{dt} = \frac{[\mathrm{OH}] - \dfrac{1}{K_2' K_3}[\mathrm{R}]}{\dfrac{1 + K_2'[\mathrm{OH}]}{k_3 K_2' [\mathrm{RH}_s]_o} + \dfrac{1}{k_4 a}\dfrac{1}{K_2' K_3}} \tag{31}$$

In this expression for the phenolic resin dissolution rate, the numerator is the driving force. The denominator, which is the overall mass-transfer resistance, includes two resistances in series. The first one is for the slow solute release, and the second one is due to solute mass transfer.

These two cases can be paralleled to find the other results given in Tables 1 and 2. We stress these two cases because they are closest to our experiments, as described below. In particular, we want to check the dissolution rates suggested by Eqs. 24 through 26 for benzoic acid, and Eq. 31 for the novolak resin. We now turn to the details of these experiments.

Experimental Studies

Materials

Sodium hydroxide (Aldrich) and benzoic acid (Fisher) were reagent grade and used as received. Phenolic resin PR 12644 was donated by the Plastics Engineering Company (Sheboygan, WI). The molecular structure of the resin was verified by ^{13}C-NMR spectroscopy (Varian INOVA 300). The resin has an average molecular weight of 2,000 g/mol, obtained by gel permeation chromatography with refractive index detection (Beckman A100, Phenomenex column with Pheno-gel MXM packing). This molecular weight value, similar to that used in photoresist formulation (Reiser, 1989), implies roughly 20 phenolic repeat units.

Apparatus

Dissolution experiments were made with a spinning disc (Levich, 1962) at room temperature. The discs, 5 cm in diameter and at least 0.5 cm thick, were contained in a stainless steel holder. Discs of benzoic acid were cast from the melt. Discs of novolak were coated in the holder as a 22% resin solution in absolute alcohol. The coated discs were oven dried to constant weight. Each disc was immersed in a 400 mL beaker containing 300 mL of aqueous sodium hydroxide and monitored with pH (model 420A pH meter, Orion). It was spun by a high-torque precision motor (Servodyne mixer head, model 50000-10; Servodyne mixer controller, model 50000-00, Cole-Parmer Instrument Co., Niles, IL). This motor has a rotation rate stability of $\pm 0.02\%$ within the range of 3–180 rpm. The upper limit of the laminar flow region ($Re = 20{,}000$) corresponds to a rotation rate of 76 rpm. Above this spinning rate, the mass-transfer coefficient is no longer given by the conventional theory of the spinning disc. Consequently, we ran our experiments between 6 and 70 rpm. Experiments were run until all the solute dissolved from the disc, but not longer than 200 min.

The concentration of dissolved solute was analyzed vs. time by UV spectrophotometry. The fiber-optic UV probe (Cary 50 Probe, Varian), synchronized with a stopwatch, took absorbance readings at 272 nm for benzoic acid or at 298 nm

Table 2. Four Cases of Dissolution with Mutiple Step Rate-Control*

Case No.	Rate-Controlling Step	Mass-Transfer Resistance $\frac{1}{Ka}$	Response to Flow (Spinning Disc)	Response to Hydroxide	Example Solute	Closest Parallel from Literature
7	S1′, S4′—Diff. in IP S3—Solute release	$\frac{l}{Da} + \frac{1 + K_2'[\mathrm{OH}]}{k_3 K_2' [RH_s]_o} + \frac{1}{D'a}\frac{1}{K_2' K_3}$	None	$\frac{1}{Ka} \propto [\mathrm{OH}]$	None known	
8	S1′—Reagent diff in IP S4′—Solute diff. in IPS4—Solute mass transfer	$\frac{l}{Da} + \frac{l}{D'a}\frac{1}{K_2' K_3} + \frac{1}{k_4 am}\frac{1}{K_2' K_3}$	$\frac{1}{Ka} \propto \frac{1}{\sqrt{Re}}$	None		
9	S3—Solute release S4—Solute mass transfer	$\frac{1 + K_2'[OH]}{k_3 K_2' [RH_s]_o} + \frac{1}{k_4 a}\frac{1}{K_2' K_3}$	$\frac{1}{Ka} \propto \frac{1}{\sqrt{Re}}$	$\frac{1}{Ka} \propto [\mathrm{OH}]$	Phenolic resin (protoresist)	Fatty acid solubilization in detergent solution (Chan et al., 1976)
10	S3—Solute release S4′—Solute diff. in IP	$\frac{1 + K_2'[\mathrm{OH}]}{k_3 K_2' [RH_s]_o} + \frac{l}{D'a}\frac{1}{K_2' K_3} + \frac{1}{k_4 am}\frac{1}{K_2' K_3}$	$\frac{1}{Ka} \propto \frac{1}{\sqrt{Re}}$	$\frac{1}{Ka} \propto [\mathrm{OH}]$		

*Case 9 is closest to our phenolic resin dissolution studies.

for the phenolic resin. Samples of *ca* 1 mL taken at the recorded times agreed with the UV absorbance readings to within one percent. To measure the saturation concentration of the solute, 2.5 to 3 g of the solid solute was stirred for several days in 17–18 g of sodium hydroxide solution. Agreement in at least triplicate was better than 2%. To find the overall mass-transfer coefficient, we first plotted the solution concentration vs. time. We found the coefficient from the equation

$$\frac{[\mathrm{R}]}{[\mathrm{R}]_{\mathrm{sat}}} = 1 - e^{-Kat} \tag{32}$$

Note that this overall coefficient implies a solute concentration difference.

Results

Determining the mechanism for mass transfer is easy with the spinning disc, because the mass transfer has a strong theoretical basis. The theory predicts that, at any radial position, the mass transfer is identical (Levich, 1962). As a corollary, the dissolving flat disc surface with negligible end-effects can be viewed as a continuous boundary moving parallel to the surface normal. In other words, the mass-transfer coefficient is the same over the entire disc's surface. This dramatically simplifies identifying the mechanism.

We found the overall mass-transfer coefficients from measurements of concentration vs. time. As expected, these follow Eq. 32, as shown in Figure 2. This figure shows typical triplicate runs under the same hydroxide and stirring conditions. The triplicate runs yield mass-transfer coefficients with less than 1.5% standard deviation. The filled points in Figure 2 refer to total surface coverage of the disc. At the smaller coverage at the end of the experiments, the concentration more slowly increases because the area of dissolving solute is reduced. We now turn to the details of these systems.

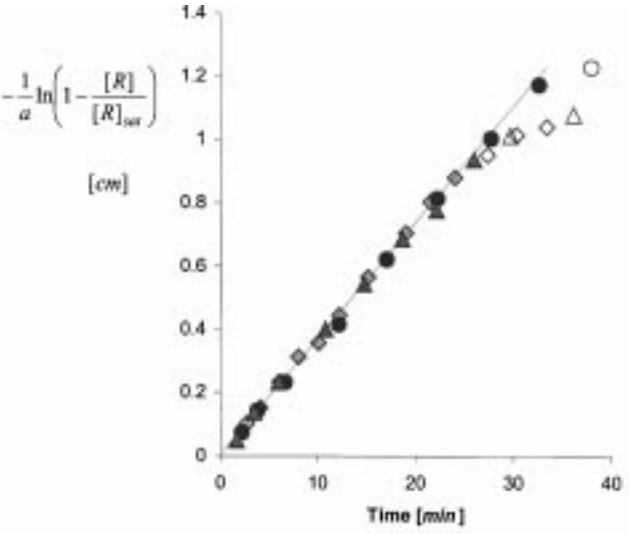

Figure 2. Typical experimental results.

This plot superimposes three independent runs (shown as squares, circles, and triangles) of phenolic resin dissolution in 0.16 mol/L NaOH with 9 rpm disc rotation rate. The filled points are results where the disc is completely covered with solute; the open points are where the disc is only partly covered. Note the reproducibility of the data; the R^2 is 0.9989.

Benzoic acid dissolution

We begin with our benzoic acid experiments, made as a benchmark for the more complex studies of the phenolic resin. In these experiments, we have three goals. First, we want to check our analysis by comparing our measured solubility with that predicted from Eq. 6. It is shown by the data at the left of Figure 3 that these closely agree. The solid line is calculated with the literature value of 4.19 for pK_a (Merck, 1996), and does not depend on adjustable parameters.

Our second goal for benzoic acid is to show that in water, the mass-transfer coefficients measured agree with those expected from the theory for the spinning disc. This theory pre-

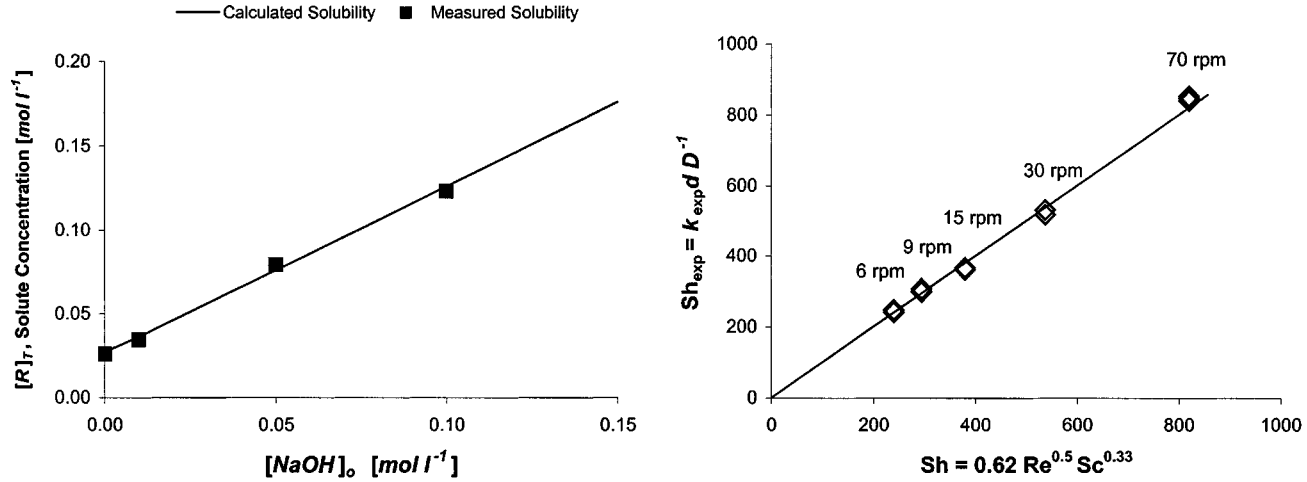

Figure 3. Experimental vs. predicted mass-transfer coefficients for benzoic acid.

The close agreement provides strong support for the accuracy of experiments with the spinning disc. The inset shows that measurements of the solubility, shown as squares, agree closely with predictions of Eq. 6 based on the acid dissociation constant and shown as the solid line.

dicts that

$$\frac{k_4 d}{D} = 0.62\left(\frac{d^2\omega}{\nu}\right)^{0.05}\left(\frac{\nu}{D}\right)^{0.33} \tag{33}$$

The data are plotted on the right of Figure 3. Again, the experimental mass-transfer coefficients, plotted as Sherwood numbers, agree closely with predictions of $k_4 d/D$, shown on the abscissa. In these calculations, we used a value of $1.0 \cdot 10^{-5}$ cm^2/s for the diffusion coefficient of benzoic acid, and a kinematic viscosity of 0.01 cm^2/s for the dilute aqueous solution.

Figure 3 shows excellent agreement between experiments and estimates. This figure does not include any adjustable parameters. This agreement verifies our expectation that mass transfer of dissolved benzoic acid is the slowest step in benzoic acid dissolution. In other words, Step 4 in the theory above is rate controlling. Although this was expected from earlier experiments with benzoic acid, it gives a simple example of the arguments that we will use for the more complex cases discussed later.

Our third goal for benzoic acid involves its dissolution in aqueous base. This case is complicated because benzoic acid and benzoate can each dissolve, and we are uncertain whether benzoate forms only at the surface or also within the boundary layer. We can try to resolve this by returning to Eq. 25, which assumes all benzoate forms at the surface, and Eq. 26, which assumes that it forms in the boundary layer. Unfortunately, both equations have the same form: they show a dissolution rate varying with a benzoic acid solubility plus a constant times the concentration of hydroxide.

We test these equations in Figure 4, which plots the measured dissolution rate vs. a collection of terms. In this collection, we know the mass-transfer coefficient k_4 from Eq. 33, the benzoic acid solubility from the inset of Figure 3, and the hydroxide concentration from our experimental conditions. We have chosen the enhancement factor E as 1.75 to give the best fit of the data. Thus, unlike Figure 3, Figure 4 does contain one adjustable parameter E.

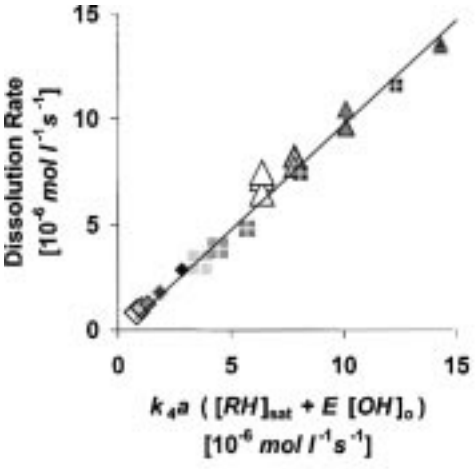

Figure 4. Dissolution rate of benzoic acid and benzoate.

The ordinate shows the experimental values, while the abscissa represents predictions based on Eq. 24 or Eq. 26. In these studies, sodium hydroxide concentration varied from 0 to 0.1 mol/L, the diamonds corresponding to distilled water, the crossed squares to 0.05 mol/L NaOH, and the triangles to 0.1 mol/L NaOH. The stirring rate changed from 6 to 70 rpm: the marker with the darker filling and the smaller size corresponds to the higher rpm.

We can come closer to the detailed mechanism by considering what the value of this parameter means. If benzoate is the dissolving species, then E is a measure of the enhanced solubility $K_2' K_3$, found from the lefthand side of Figure 3 to equal 1.0. If benzoate forms only in solution, then E is a

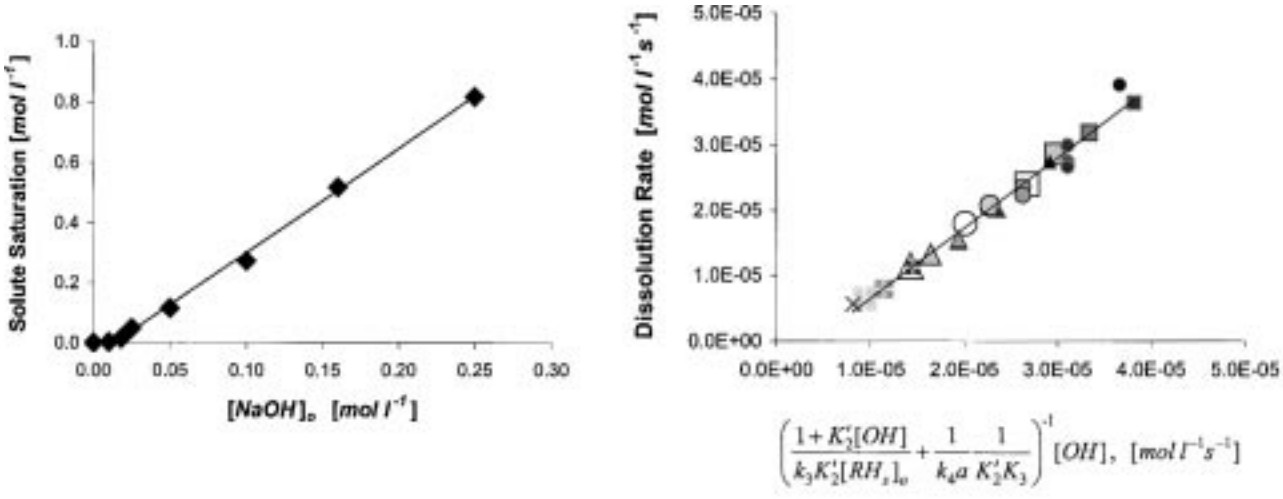

Figure 5. Dissolution rate of phenolic resin.

As in Figure 4, the ordinate shows the experimental values, while now the abscissa has predictions from Eq. 31. These predictions include values of 10^4 m$^{-1}\cdot$s^{-1} for k_3 and 0.10 mol/L for K_3. The hydroxide concentration ranges from 0.025 to 0.25 mol/L, with the "x" corresponding to 0.025 mol/L NaOH, the crossed squares to 0.05 mol/L, the triangles to 0.1 mol/L, the circles to 0.16 mol/L, and the plain squares to 0.25 mol/L NaOH. The spinning rate of the disc varied from 6 to 70 rpm: again the marker with the darker filling and the smaller size corresponds to the higher rpm. The inset gives resin solubility vs. sodium hydroxide concentration.

ratio of the two-thirds power of the diffusion coefficients $(D_{NaOH}/D_{RH})^{2/3}$ or $(2.12/1.00)^{2/3} = 1.66$ (Cussler, 1997). This is close to the experimental value of 1.75, suggesting that the reaction forming benzoate is in solution, not at the surface.

Photoresist dissolution

We now turn to the dissolution of the majority component of the photoresist: the phenolic resin. We compared our data with all of the mechanisms summarized in Tables 1 and 2, and found the data were best described by Case 9. This case, which assumes both solute release and mass transfer can be rate-limiting steps, was developed in detail in the theory section above. It led to the dissolution rate given by Eq. 31.

We want to show that this result is consistent with our experiments. To do so involves discussing seven parameters. Only a synopsis of this discussion is given here, since details were given elsewhere (Hunek, 2000). First, we made our experiments under conditions where the concentration of dissolved phenolic resin [R] was small, so the second term of the numerator in Eq. 31 can be neglected. Secondly, we took the equilibrium constant K_2' as equal to the dissociation constant of the phenolic group, a group with a pK_a of 12.4 (Flanagin et al., 1999). Thirdly, we estimated the concentration $[RH]_o$ from the resin density of 1.3 g/cm^3, the repeat unit molecular weight of 106 g/mol, and an expected surface dimension of 5Å×5Å. Fourth, we again used Eq. 33 to find k_4, based on a diffusion coefficient of $2 \cdot 10^{-6}$ cm^2/s for the resin.

We still do not know the rate constant of solute release from the solid phase k_3 or the corresponding equilibrium constant K_3. These quantities remain unknown. The first appears in the resistance due to slow solute release, which also includes the effect of hydroxide. The second appears in the resistance to mass transfer in solution. We must determine both these quantities from experiment.

Our results for phenolic resin dissolution are shown in Figure 5. The lefthand side of the figure gives the solubility of the resin vs. hydroxide concentration, which is close to linear. The actual dissolution rates, shown in the righthand side of the figure, are correlated with the expected collection of variables suggested by Eq. 31. In this correlation, we have taken k_3 as 10^4 m$^{-1}\cdot$s^{-1} and K_3 as 0.10 mol/L. With these two parameters, we correlate all the results, including base concentrations from 0.025 to 0.25 mol/L and stirring speeds from 6 to 70 rpm. We will explore the physical meaning of the results in the discussion section.

Discussion

In the above, we report dissolution rates which we studied experimentally. The first, simpler case of benzoic acid is controlled by solute mass transfer. The second phenolic resin case is limited by a combination of solute release and mass transfer. In this section, we first compare these mechanisms to show their experimental differences. We then discuss how to extend our results to other studies of photoresist dissolution.

Comparing the dissolution mechanisms

One easy method of comparison, often used in studies of dissolution, is in terms of an overall mass-transfer coefficient,

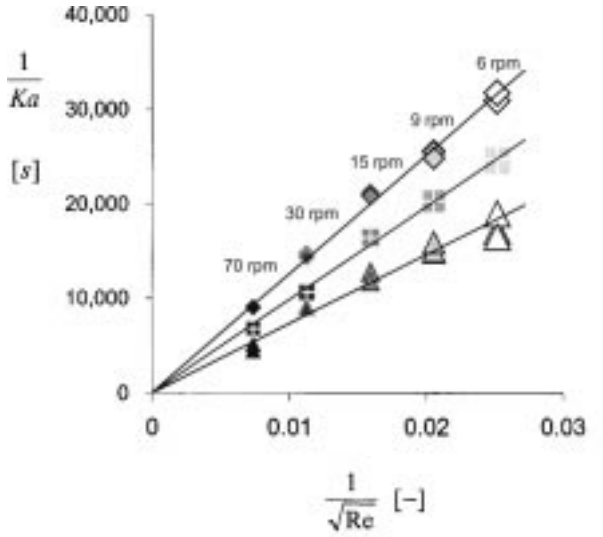

Figure 6. Wilson plot for benzoic acid dissolution.

The zero intercept on this plot, corresponding to infinite flow, implies that any surface reactions are much faster than transport in solution. Sodium hydroxide concentration varied from 0 to 0.1 mol/L, while the stirring rate changed from 6 to 70 rpm. The marker with the darker filling and the smaller size corresponds to the higher rpm. As in Figure 4, the diamonds correspond to distilled water, the crossed squares to 0.05 mol/L NaOH, and the triangles to 0.1 mol/L NaOH.

defined at small times by

$$\frac{d[\mathrm{R}]}{dt} = Ka[\mathrm{OH}] \tag{34}$$

A higher hydroxide concentration gives a higher solubility, and so should give a higher dissolution rate expressed as K. One easy way to summarize values of K, often called a Wilson plot, shows the reciprocal of the mass-transfer coefficient vs. the reciprocal of some power of the Reynolds number. For the spinning disc, the power is 0.5 (Levich, 1962). Such a plot has both a slope and an intercept. The slope signals the varying importance of the resistance in solution: a large slope indicates a large solution resistance. The intercept is more subtle. Because the flow increases in the negative direction on the abscissa, the limit of infinite flow is at the zero of the abscissa. Hence, the intercept of such a plot gives the mass-transfer resistance which is not due to solution but to processes at the interface. A zero intercept means fast interfacial processes.

The Wilson plot for the dissolution of benzoic acid is shown in Figure 6. It shows exactly what we would expect for this dissolution. Since the intercept is zero, all interfacial processes, such as acid-base reaction and solute release, are fast. The only mass-transfer resistance comes from the slow solute mass transfer. Because this step takes place in the interfacial liquid, this mass-transfer resistance diminishes as the Reynolds number becomes large. As we would expect, the mass-transfer resistance decreases with increasing hydroxide concentration.

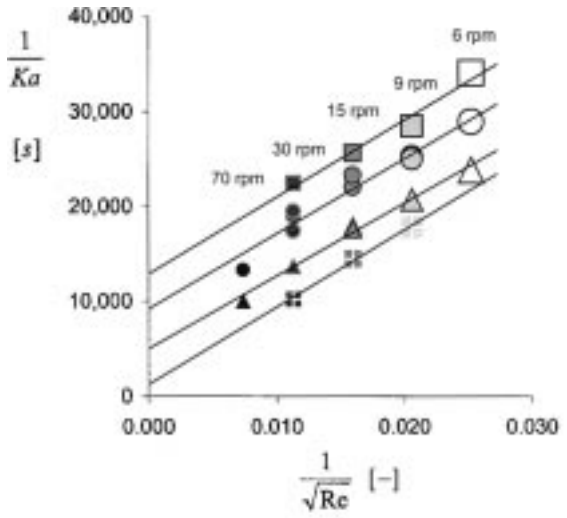

Figure 7. Wilson plot for phenolic resin dissolution.

The positive intercepts at infinite flow indicate that the dissolution sequence includes a slow surface process before slow solute mass transfer. As in Figure 5, the crossed squares correspond to 0.05 mol/L NaOH, the triangles to 0.1 mol/L, the circles to 0.16 mol/L, and the plain squares to 0.25 mol/L NaOH.

The Wilson plot for phenolic resin dissolution, shown in Figure 7, is different from that for benzoic acid. Now, the values at different hydroxide concentrations extrapolate to finite intercepts. The values of these intercepts, corresponding to the resistances at infinite flow, *increase* as the hydroxide concentration increases. However, the slopes on the Wilson plot are all nearly equal, suggesting that the resistance in solution is nearly the same.

The key dissolution steps for the resin, consistent with solute release from the solid surface and mass transfer in solution, are contrasted with those for benzoic acid by the cartoons in Figure 8. The results for benzoic acid are as expected. The results for the resin surprisingly show the increased intercepts at *higher* base concentrations. This occurs because the reacted solute must uncover another unreacted solute as it is released from the surface (cf. Eq. 16). If the hydroxide concentration gets higher, the rate of this step approaches an asymptote because this interfacial process depends solely on the interaction between polymer segments. However, because of its definition in Eq. 34, K decreases as hydroxide increases. This causes the observed behavior.

Comparing dissolution of polymers, including photoresists

Finally, we turn to comparing our results with those suggested by other experiments. We can make this comparison in three ways. First, we note that our studies always show a variation of dissolution with solution flow. This means that mass transfer in solution is always involved in the dissolution rates. This is consistent with dissolution measurements of other dissolving polymers, including some lithographic inks (Bhaskarwar and Cussler, 1997). The variation with flow has often been neglected in studies of photoresist dissolution, which makes determining the detailed mechanism difficult.

Secondly, our studies show no evidence of an intermediate phase. This is in contrast with the lithographic inks and with some earlier photoresist studies, but supports the findings of

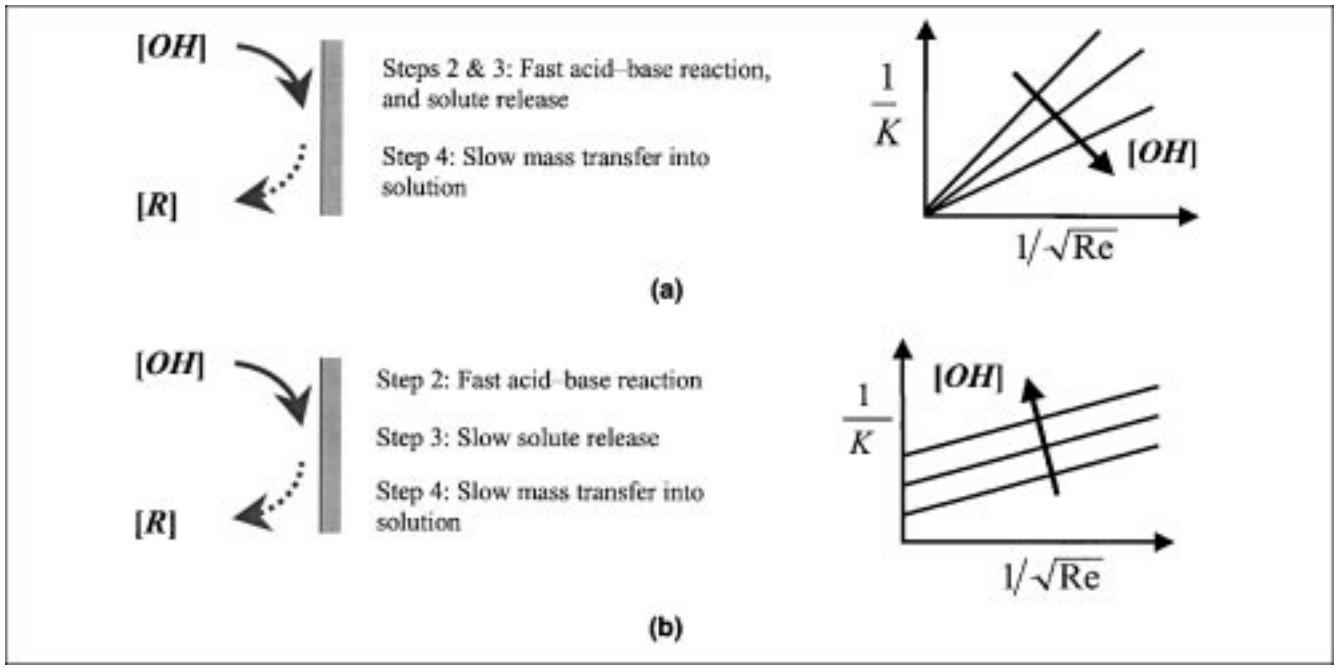

Figure 8. Cartoons and Wilson plots for benzoic acid and phenolic resin dissolutions.

(a) Cartoon of benzoic acid dissolution, and the corresponding Wilson Plot; (b) cartoon of phenolic resin dissolution with the schematic Wilson plot.

Tsiartas et al. (1997). The inks actually had the intermediate phase, which sheared off, transferring the substrate into the solution. However, although the possibility of an intermediate phase is included in the analysis summarized in Tables 1 and 2, we did not observe it in our experiments. This is consistent with expectations for this dissolving system, because the polymer has approximately 20 repeat units, which is well below the entanglement limit (Tsiartas et al., 1997). In addition, the low molecular weight causes a low upper critical solution temperature, which limits the temperature range of stability for the intermediate phase.

Third, our results are consistent with those of Tsiartas et al. (1997) in highlighting the key role chemical reaction plays in phenolic resin dissolution. Our modeling efforts take this role further. Since both base diffusion to the reaction front and acid-base reaction (Steps 1 and 2) are fast, ionization approaches equilibrium at the solid resin surface. However, the Wilson plot for the phenolic resin (Figure 7) indicates that before slow solute mass transfer, there is a step in the dissolution sequence that involves a slow surface process. We believe this key step is the hindered release of the soluble phenolate ionic segments from the solid phenolic polymer phase (Step 3). This hindered release is similar to that of water soluble polymers, such as xanthan or pectin (Parker et al., 2000), although it occurs without the formation of a "gel layer." This release was not found to be slow during the dissolution of benzoic acid. Therefore, the key chemical difference between phenolic resins and benzoic acid, that is, the presence of a polymer backbone connecting the ionized units, is responsible for this hindered solute release.

"Strings of buoys" analogy for dissolution

In conclusion, we can summarize the relevant dissolution mechanisms based on a simple analogy. Imagine a swimming pool of solvent where untied lane markers float freely. A lane marker, essentially a small buoy on a string, can be viewed as a model of a polymer molecule: the buoys represent the repeat units, and the string provides the polymer backbone. If the solvent is now removed from the swimming pool, the lane markers collapse to the bottom to form a "solid phase." This "phase" will be a highly entangled mess unless the strings of buoys are very short. In other words, the degree of entanglement depends on the length of strings, corresponding to polymer molecular weight. In the remainder of this article, three dissolution cases are described and rationalized by drawing analogies between dissolution and dissolving "strings of buoys" in a pool of solvent.

First, we consider the case of long strings of "lane markers," which is analogous to the dissolution of high molecular weight soluble polymers above the entanglement limit. After filling the pool, the solvent penetrates the entangled mess of the "solid phase" of buoys because of gravity, which suggests the affinity of solvent to the soluble solute. The buoyancy of the lane marker buoys, which represents the solubility driving the solute to dissolve in the solvent, causes the formation of a swollen zone, that is, a "gel layer." However, the disentanglement and release of the physically entrapped strings of buoys is slow, which results in a significant resistance to dissolution. For large polymer molecules, such as xanthan or pectin, this resistance to the release of "polymer chains" can be so significant that it may dwarf the resistance to the diffusion of the large and thus sluggish solute. Hence, the key dissolution rate-limiting step is the release of solute from the solid or gel phase (Parker et al., 2000).

The second analogy describes the dissolution of short strings of buoys that model small soluble polymers well below the entanglement molecular weight. This case also includes the dissolution of individual buoys without strings, corresponding to simple, nonpolymeric solutes, such as benzoic acid. In this case, the release of the buoys is significantly accelerated due to the lack of entanglement. Here, the rate-controlling process is solute diffusion alone, as in the case of simple solutes.

Thirdly, we consider the case of the dissolution of short strings of "lane markers," that is, polymers well below the entanglement molecular weight, but now significant solute-solute and solute-solvent interactions complicate the physical situation. This case includes the dissolution of low molecular weight phenolic resins in aqueous base, the centerpiece of this work. To extend our "string of buoys" analogy to this case, three special features of phenolic resin dissolution need to be incorporated. To begin, the unionized phenolic polymer is insoluble, so the buoyancy is zero. In addition, adjacent phenolic groups cause attractive solute-solute interactions between the "buoy repeat units," for example, through hydrogen bonding. Finally, reaction with base restores the buoyancy by overcoming this interaction.

With this modified "strings of buoys" analogy, we can rationalize the key features of the resin dissolution as follows. When we add base on top of a layer of "lane markers" without buoyancy, we do not expect "gel layer" formation because the "strings of buoys" are not soluble. In addition, the interactions hold together the buoy repeat units of different strings. As the base is transferred to the interface, the reaction quickly makes some buoys buoyant, while unreacted buoys are still trapped in the "solid" phase. Reacted individual buoys trying to leave the "lane marker" phase cannot because of the unreacted, trapped buoys connected to them. The result is the same as in the first analogy: Step 3, the release of the strings is hindered, although the reason is solute-solute interaction, not entanglement. After a sufficient fraction of buoys is reacted on the same string, the large, sluggish string slowly transfers into the bulk solvent by diffusion (Step 4). These last two steps are comparably slow, so their combination controls the rate of dissolution. This theory is consistent with the results of our phenolic resin dissolution experiments.

These analogies provide a simple rationalization for the different dissolution mechanisms at work. Our analogy of "strings of buoys" could be extended to other dissolution cases as well, but we believe that the above cases give a comprehensive summary of the most relevant dissolution mechanisms that we have focused on in this article.

Acknowledgment

This work was largely supported by the National Science Foundation (Grant CTS 94-28755). Other support came from the National Science Foundation (CTS 96-27361) and the Department of Defense (F49620-01-1-0333). We thank Ms. Melanie M. Choe for carefully performing some of the benzoic acid dissolution experiments.

Notation

a = dissolving surface area to solution volume ratio, L^{-1}
d = diameter of the disc, L
D = diffusion coefficient, $L^2 \cdot t^{-1}$
E = enhancement factor due to chemical reaction
k = mass-transfer coefficient, $L \cdot t^{-1}$
k_1 = hydroxide mass-transfer coefficient (Step 1), $L \cdot t^{-1}$
k_2 = forward acid-base surface reaction rate constant, $L^2 \cdot \text{mol}^{-1} \cdot t^{-1}$
k_{-2} = reverse acid-base surface reaction rate constant, $L^2 \cdot \text{mol}^{-1} \cdot t^{-1}$
k_3 = rate constant of solute release from solid surface, $L^{-1} \cdot t^{-1}$
k_{-3} = rate constant of solute readsorption back to solid surface, $L^2 \cdot \text{mol}^{-1} \cdot t^{-1}$
k_4 = solute mass-transfer coefficient (Step 4), $L \cdot t^{-1}$
K = overall mass-transfer coefficient, $L \cdot t^{-1}$
K_2 = acid-base reaction equilibrium constant (Step 2)
$K_2' = K_2/[H_2O]$ = modified acid-base reaction equilibrium constant (Step 2), $L^3 \cdot \text{mol}^{-1}$
K_3 = equilibrium constant of solute release (Step 3), $\text{mol} \cdot L^{-3}$
K_a = acid dissociation constant, $\text{mol} \cdot L^{-3}$
K_w = water self-dissociation constant, $\text{mol}^2 \cdot L^{-6}$
l = thickness of intermediate solute-rich phase, L
m = partition coefficient
r = rate of a step, $\text{mol} \cdot L^{-3} \cdot t^{-1}$
Re = Reynolds number
t = time, t
ν = kinematic viscosity, $L^2 \cdot t^{-1}$
ω = rotation rate, $\text{rad} \cdot t^{-1}$

Subscripts

i = at the interface adjacent to the liquid solution phase
o = at zero time: before dissolution
s = at acid-base reaction front (implies surface concentration), $\text{mol} \cdot L^{-2}$
sat = saturation
T = total

Literature Cited

Arcus, R. A., "A Membrane Model for Positive Photoresist Development," *Proc. SPIE*, **631**, 124 (1986).

Atkins, P. W., D. F. Shriver, and C. H. Langford, *Inorganic Chemistry*, Freeman, Oxford (1995).

Bhaskarwar, A. N., and E. L. Cussler, "Pollution-Preventing Lithographic Inks," *Chem. Eng. Sci.*, **52**, 3227 (1997).

Chan, A. F., D. F. Evans, and E. L. Cussler, "Explaining Solubilization Kinetics," *AIChE J.*, **22**, 1006 (1976).

Cussler, E. L., *Diffusion: Mass Transfer in Fluid Systems*, Cambridge University Press, Cambridge (1997).

Flanagin, L. W., C. L. McAdams, W. D. Hinsberg, I. C. Sanchez, and C. G. Willson, "Mechanism of Phenolic Polymer Dissolution: Importance of Acid-base Equilibria," *Macromol.*, **32**, 5337 (1999).

Fredd, C. N., and H. S. Fogler, "The Kinetics of Calcite Dissolution in Acetic Acid Solutions," *Chem. Eng. Sci.*, **53**, 3863 (1998).

Grant, C. S., A. T. Perka, W. D. Thomas, and R. Caton, "Cleaning of Solid Behenic Acid Residue from Stainless-Steel Surfaces," *AIChE J.*, **42**, 1465 (1996).

Han, Y. K., and A. Reiser, "Length of Phenolic Strings in Dissolution Inhibition Resists," *Macromol.*, **31**, 8789 (1998).

Hunek, B., "Mechanism of Photoresist Dissolution," PhD Thesis, Univ. of Minnesota, Minneapolis (2000).

Kabin, J. A., A. E. Sáez, C. S. Grant, and R. G. Carbonell, "Removal of Organic Films from Rotating Disks Using Aqueous Solutions of Nonionic Surfactants: Film Morphology and Cleaning Mechanisms," *Ind. Eng. Chem. Res.*, **35**, 4494 (1996).

Levich, V. G., *Physicochemical Hydrodynamics*, Prentice Hall, Englewood Cliffs (1962).

Littlejohn, F., C. S. Grant, and A. E. Sáez, "Mechanisms for the Removal of Calcium Phosphate Deposits in Turbulent Flow," *Ind. Eng. Chem. Res.*, **39**, 933 (2000).

Merck & Co., Inc., *Merck Index*, Whitehouse Station, NJ (1996).

Parker, A., F. Vigouroux, and W. F. Reed, "Dissolution Kinetics of Polymer Powders," *AIChE J.*, **46**, 1290 (2000).

Peppas, N. A., J. C. Wu, and E. D. von Meerwall, "Mathematical Modeling and Experimental Characterization of Polymer Dissolution," *Macromol.*, **27**, 5626 (1994).

Permsukarome, P., C. Chang, and H. S. Fogler, "Kinetic Study of Asphaltene Dissolution in Amphiphile/Alkane Solutions," *Ind. Eng. Chem. Res.*, **36**, 3960 (1997).

Reiser, A., *Photoreactive Polymers: the Science and Technology of Resists*, Wiley Interscience, New York (1989).

Reiser, A., H. Y. Shih, T. F. Yeh, and J. P. Huang, "Novolak-Diazoquinone Resists — The Imaging Systems of the Computer Chip," *Angew. Chem. Int. Ed. Engl.*, **35**, 2428 (1996).

Robertson, E. A., III, and H. S. Fogler, "Model for the Reaction-Rate-Limited Dissolution of Solids with Etch-Rate Heterogeneities," *AIChE J.*, **42**, 2654 (1996).

Tsiartas, P. C., L. W. Flanagin, C. L. Henderson, W. D. Hinsberg, I. C. Sanchez, R. T. Bonnecaze, and C. G. Willson, "The Mechanisms of Phenolic Polymer Dissolution: A New Perspective," *Macromol.*, **30**, 4656 (1997).

Manuscript received Mar. 29, 2001, and revision received Oct. 23, 2001.